Electronic Supplementary Material (ESI) for Nanoscale.

Supplementary Material:

Temperature Dependence of the Radiative Lifetimes in Ge and Si Nanocrystals

Nancy C. Forero-Martinez[1], Ha-Linh Thi Le[1], Ning Ning[1], Holger Vach[1], and H.-Ch. Weissker[2,3]

[1] LPICM, Ecole Polytechnique, CNRS, 91128 Palaiseau, France.
[2] Aix Marseille University, CNRS, CINaM UMR 7325, 13288, Marseille, France
[3] European Theoretical Spectroscopy Facility

Saturday 6th December, 2014

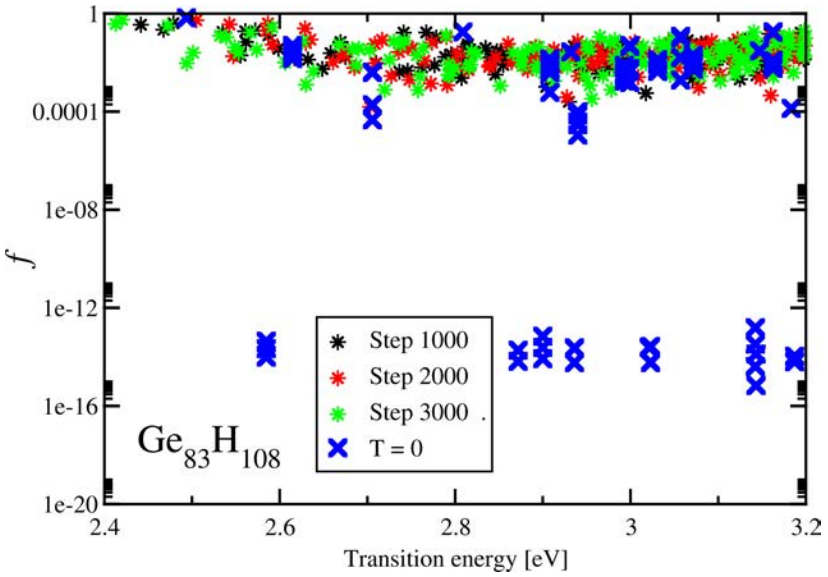

Figure S1: Kohn-Sham calculations: Oscillator strengths and energies based on the Kohn-Sham system, calculated for the lowest transitions of the fully saturated $Ge_{83}H_{108}$ at $T = 0$ and for the three snapshots out of the trajectory at 100 K. At $T = 0$ (rigid lattice), the HOMO-LUMO transition is by far the strongest. In general, at $T = 0$ the transitions are separated into strong transitions and clearly forbidden transitions. On the other hand, during the vibration, the formerly degenerate HOMO-LUMO transition is split and the respective single transitions are all somewhat weaker, as a sign that the loss of full symmetry weakens the transitions. Moreover, the oscillator strengths lie in a much narrower range. In particular, the HOMO-LUMO transition is weaker and the degeneracy slightly lifted.

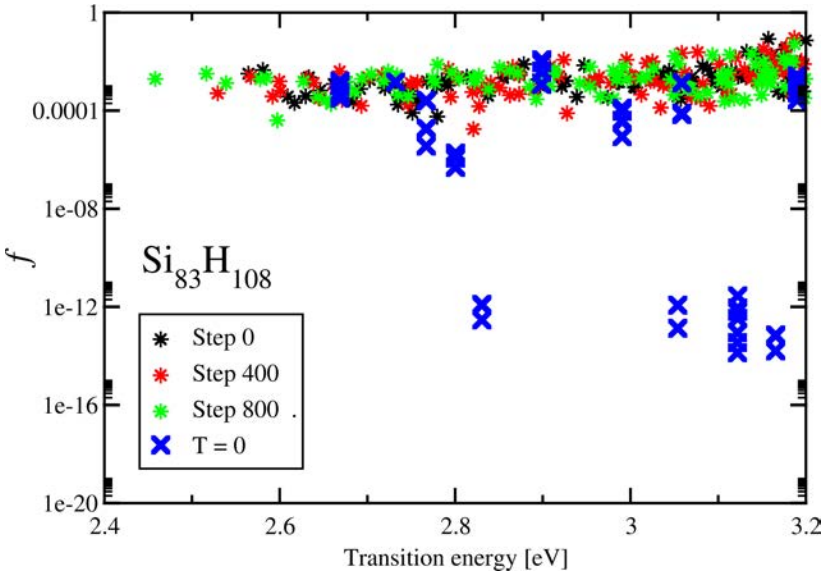

Figure S2: Kohn-Sham calculations: transition energies and oscillator strengths as in Fig. S1 for $Si_{83}H_{108}$. At $T = 0$, the threefold degenerate HOMO-LUMO transition is rather weak (almost three orders of magnitude weaker than in $Ge_{83}H_{108}$). Moreover, there is a large number of weak and very weak transitions. The changes during the vibration fluctuate; on average, the transition probability increases. Unlike in $Ge_{83}H_{108}$, at least some of the low-energy transitions become stronger than the HOMO-LUMO transition at $T = 0$.

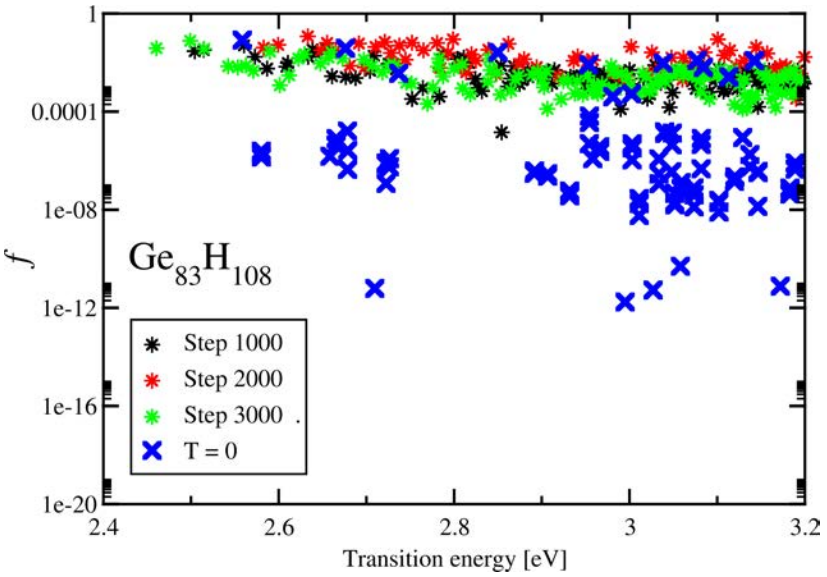

Figure S3: TDDFT transition energies and oscillator strengths of the lowest transitions of the fully saturated $Ge_{83}H_{108}$ at $T = 0$ and for the same three snapshots out of the trajectory at 100 K shown in Fig. S1. The LDA/ALDA results have been calculated in TDDFT using Casida's approach as implemented in the octopus code. The spacing was set to 0.20 Å and the radius of the spheres that make up to simulation domain to 6.0 Å. For the calculation of the transitions aroung the gap, 40 occupied and 40 unoccupied states were used in the Casida calculation. While the numbers are somewhat different from those based on the Kohn-Sham system (Fig. S1), the conclusions are exactly the same.

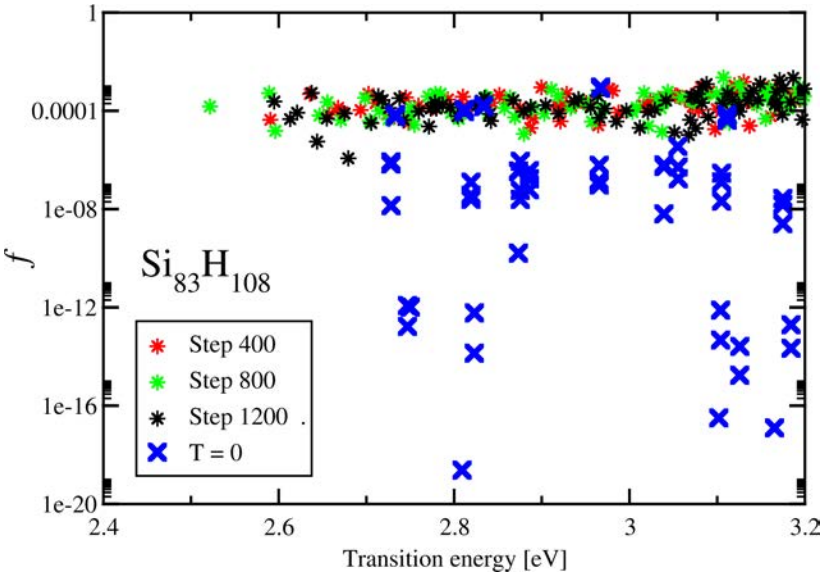

Figure S4: TDDFT transition energies and oscillator strengths as in Fig. S3 for $Si_{83}H_{108}$. While the numbers are somewhat different from those based on the Kohn-Sham system (Fig. S2), the conclusions are exactly the same.

Expression of the oscillator strengths as used in eq. (1) of the article

The DFT calculation has been carried out using the supercell method, i.e., with an artificial periodicity. The the oscillator strengths are

$$f_{cv} = \sum_{\alpha} f_{cv}^{\alpha\alpha}(\mathbf{k}) = \frac{2m \left|\langle c\mathbf{k} \left|\hat{v}_\alpha\right| v\mathbf{k}\rangle\right|^2}{\varepsilon_c(\mathbf{k}) - \varepsilon_v(\mathbf{k})} \tag{1}$$

where $\hat{v}_\alpha$ is the velocity operator ($\alpha = x, y, z$). Only one $\mathbf{k}$ point is used ($\mathbf{k} = 0$, i.e., Γ). We thus include optical transitions between valence (occupied) ($|v\mathbf{k}\rangle$) and conduction (unoccupied) ($|c\mathbf{k}\rangle$) states.

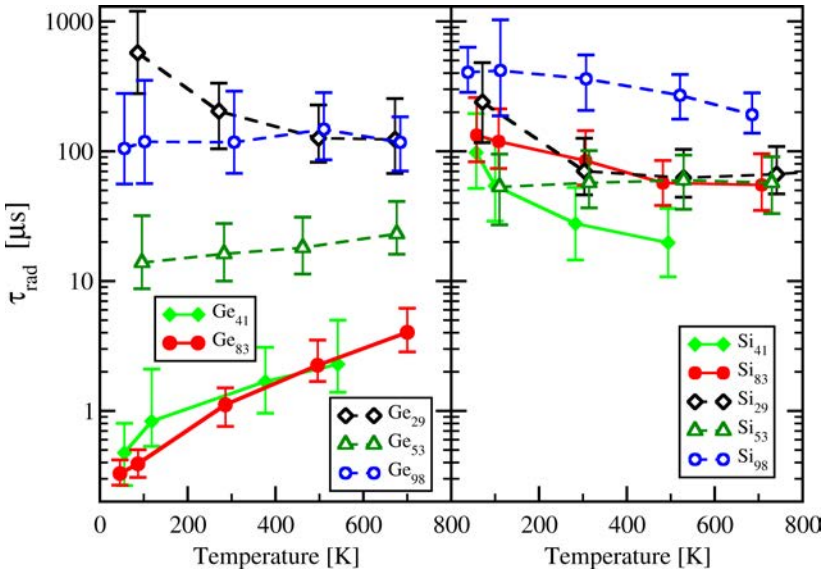

Figure S5: Radiative lifetimes as in Fig. (1) and (3) of the manuscript. We show the median of the distribution of the lifetimes over the trajectory, which is rather unsymmetric. The bars mark the 25 % and 75 % percentiles of the distribution and thus indicate the spread of the values in the sample. Note that this is *not* a confidence interval for the sample lifetime values but information on the width of the distribution.

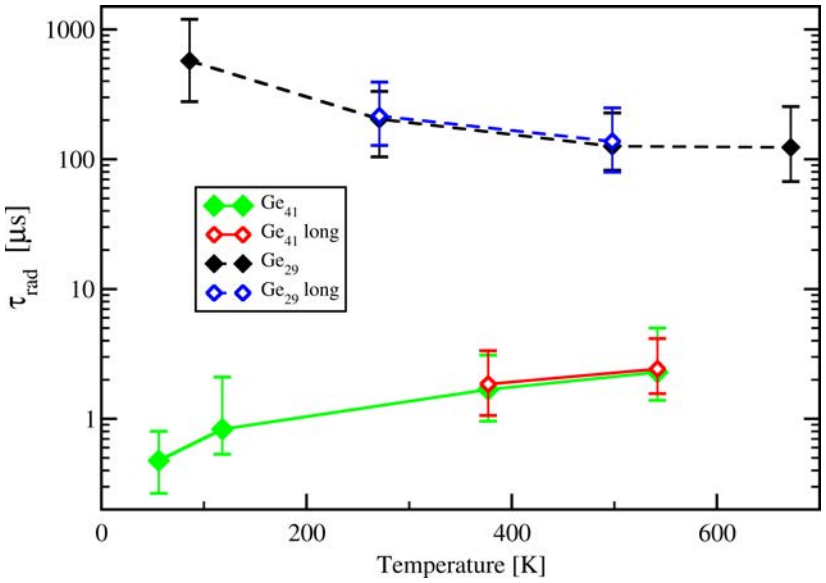

Figure S6: In order to verify the quality of our calculations, we compare the values as calculated using the 5 ps trajectories (the time span used in all the calculations presented in the paper) with longer runs of 20 ps for two temperature values each: Ge_{29} and Ge_{41}. For Ge_{29}, we collected 1000 snapshots (ten times the original number). For Ge_{41}, we multiplied both the time and the number of snapshots by 4 (400 snapshots, 20 ps). The comparison with the original calculation shows very close agreement between the two calculations which perfectly demonstrates the validity of the statistical sampling we have carried out.

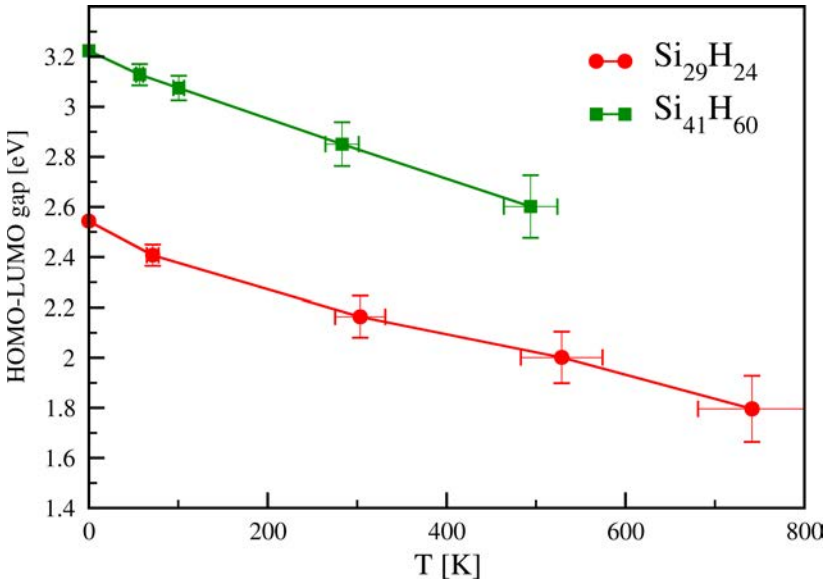

Figure S7: The HOMO-LUMO gaps of two of the Si NCs shown as a consistency check of our calculation. The decrease is consistent with numerous experiments as well as with the calculations of Franceschetti [Phys. Rev. B, **76,** 161301 (2007)] where the same approach to include classical temperature effects has been used.

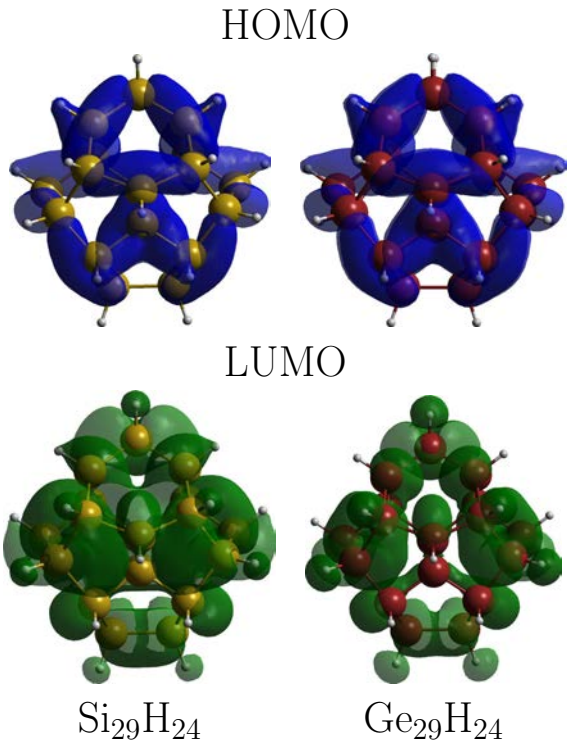

Figure S8: HOMO and LUMO states ($|\psi|^2$ at 10 % of the maximum value) of the "reconstructed" $Ge_{29}H_{24}$ and $Si_{29}H_{24}$.

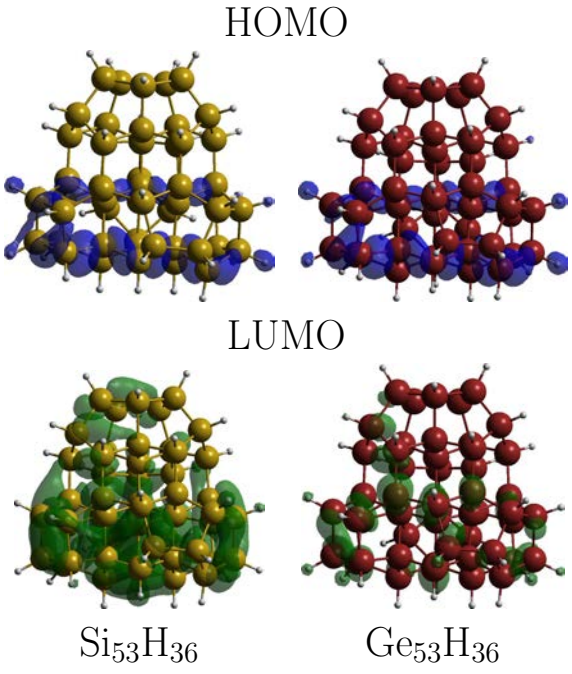

Figure S9: HOMO and LUMO states ($|\psi|^2$ at 10 % of the maximum value) of the "reconstructed" $Ge_{53}H_{36}$ and $Si_{53}H_{36}$.